nzsee
NEW ZEALAND SOCIETY FOR EARTHQUAKE ENGINEERING

# Lower and upper design limit force estimation for lead extrusion damper: A classical extrusion modelling approach

*V. Vishnupriya & G.W. Rodgers*
Department of Mechanical Engineering, University of Canterbury, Christchurch and QuakeCoRE: NZ Centre for Earthquake Resilience, Christchurch

*J.G. Chase*
Department of Mechanical Engineering, University of Canterbury, Christchurch

## ABSTRACT

To reduce seismic vulnerability and the economic impact of seismic structural damage, it is important to protect structures using supplemental energy dissipation devices. High force to volume (HF2V) devices are supplemental energy dissipation devices with a small volumetric size and with high force capacities. HF2V devices have previously been designed using very simple models with limited precision. They are manufactured, and tested to ensure force capacities match design goals, potentially necessitating reassembly or redesign if the force deviates from the desired design value. Thus, there is a need for a modelling methodology to accurately estimate the range of possible device force capacity values in the design phase.

Upper bound (UB) and lower bound (LB) force capacity estimates are developed from equations in the metal extrusion literature. These equations consider both friction and extrusion forces between the lead and the bulged shaft in HF2V devices. The equations for the lower and upper bounds are strictly functions of device design parameters ensuring easy use in the design phase. The models are validated by comparing the bounds with experimental force capacity data from experimental testing on 15HF2V devices.

All lower bound estimates ($F_{LB}$) are below the experimental device forces, and all upper bound ($F_{UB,\ indirect}$) estimates are above. Precise HF2V device design forces are calculated by taking the mean of LB and UB model forces and compared to experimental forces. The HF2V device forces are predicted within an error of 1-16%. Therefore, these modelling methods provide a useful design tool.

## 1 INTRODUCTION

Earthquakes can occur regularly in seismically active areas. The social and economic after effects of a seismic event may be severe, leaving lasting socioeconomic (Amini Hosseini et al., 2013; King et al., 1997;

Shinozuka et al., 1998) and psychological impact (Dorahy et al., 2016; Xu et al., 2012) on the society. Lead extrusion dampers (LED) are supplemental energy devices utilizing the hysteretic properties of lead to reduce response of a structure to earthquake loading. HF2V dampers are prestressed lead extrusion dampers with smaller volume and higher force capacity. Dampers using this broad design date back to the 1970s (Robinson and Grenbank, 1976; Cousins and Porritt, 1993), have been tested previously with reinforced concrete (Rodgers et al, 2012, 2016), steel (Mander et al, 2009), and timber connections (Wrzesniak, 2016). This damping method has also found satisfactory applications in Christchurch rebuild with 96 applied in the Forté Health (D. Latham et al., 2013; D. A. Latham et al., 2013; Rodgers, 2019) and 20 more in the new Christchurch Library (Tūranga) (Shannon, 2019).

The specific design force and displacement capacity requirements for a damper for a given structure will depend upon a number of structural design parameters. Therefore, there is a need to be able to reliably predict damping device forces for any given required force capacity. Having methods able to predict upper and lower bounds of the final device performance will eliminate the need for iterative design and experimental testing to achieve a final desired device performance. While previous research has developed a detailed non-linear finite element method to predict response forces (Vishnupriya, 2020) and an empirical model to predict design forces (Vishnupriya et al., 2018), this paper investigates a simpler first-principles hand analysis that may be able to offer similar accuracy with much less computational effort.

Due to the inherent complexity of the extrusion process, exact prediction of extrusion forces can be difficult. Upper bound (UB) theorems estimate maximum forces based on yield criteria and geometric self-consistency. Lower bound (LB) theorems determine the minimum forces produced, neglecting geometric self-consistency (Drucker et al., 1952; Hosford, 2007).

## 2 HF2V LB EQUATION ($F_{LB}$)

Lower bound extrusion forces can be estimated based on work models used to obtain metalworking loads, which assumes homogenous deformation and zero friction (Horrobin & Nedderman, 1998; Rowe, 1979; Symons et al., 2014):

$$F_{LB,extrusion} = A_o Y_o' \ln\frac{A_o}{A_f} \quad (1)$$

Where, $Y_o$ is the yield stress, $A_o$ is the area of lead before extrusion, and $A_f$ is the lead area after extrusion. This model assumes pure extrusion with ideal deformation, no friction and no redundant work (Groover, 2013; Horrobin & Nedderman, 1998). Thus, the friction force between the steel parts and lead is neglected. However, from previous research the overall HF2V device of the overall lower bound force developed in the HF2V damper can be obtained by adding the frictional force component for the entire shaft is added to Equation (1):

$$F_{LB} = A_o Y_o \ln\frac{A_o}{A_f} + m\pi D_{sh}\frac{Y_o}{\sqrt{3}}L_{cyl} \quad (2)$$

Where, $m$ is the friction factor, $D_{sh}$ is shaft diameter, $L_{cyl}$ is the length of the cylinder.

## 3 INDIRECT EXTRUSION ANALOGY

In indirect metal forming processes, a stamp head is forced through the working material by compressing and shearing the working material and pushing it in the opposite direction to the direction of displacement of stamp. The extrusion process in an HF2V damper is similar where in a closed steel container the working material (lead) is extruded by the bulge and forced to flow against the shaft behind the bulge (Rodgers, 2009). The overall geometry in the indirect extrusion case is similar to the geometry of the HF2V devices seen in Figure 1. The bulges in the HF2V devices are analogous to the stamp head in indirect extrusion

processes and the cylinder walls are comparable to the container walls. The functions of the bulge, stamp head and die are to deform the metal during the extrusion process. Compression and shear forces are produced from deformation of metal and friction between the metal and moving parts in both the processes.

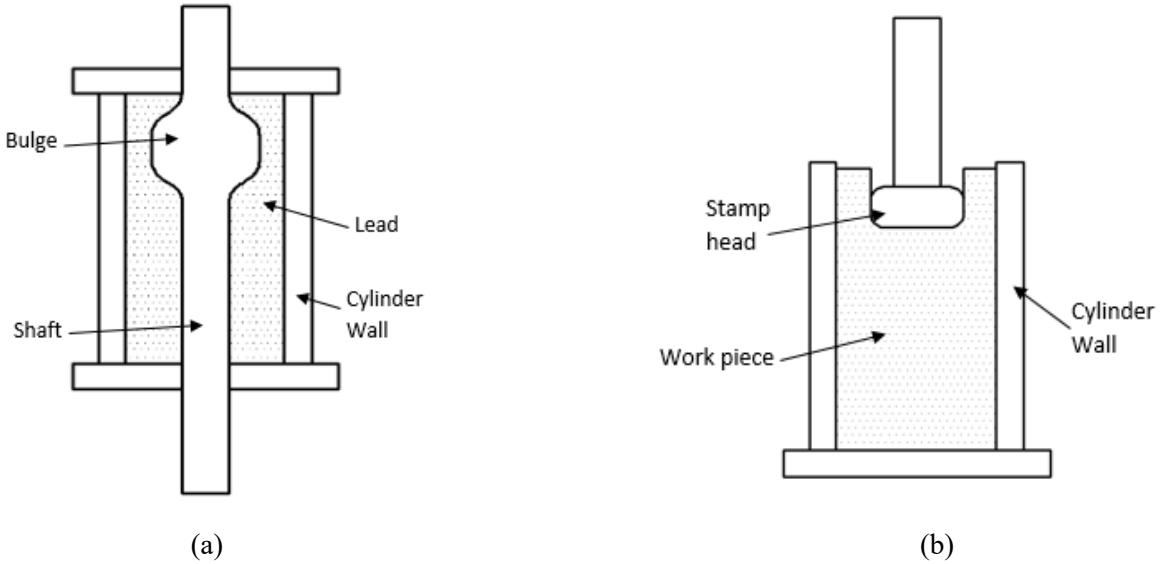


(a) (b)

Figure 1: (a) HF2V parts (b) Indirect extrusion parts

### 3.1 HF2V indirect extrusion UB modelling

A constitutive approach is considered for indirect extrusion force modelling, where the sum of forces dissipated in the extrusion process is considered. The forces produced by indirect extrusion are from friction between the work piece-stamp ($F_p$), workpiece- cylinder wall ($F_m$), compression of the work piece ($F_r$) and deformation of work piece ($F_{def}$) (Socaciu, 2014), defined:

$$F_i = F_p + F_m + F_r + F_{def}$$

$$= \left(8\mu k \cdot \frac{h_p}{d} \frac{D^2}{D^2 - d^2} \cdot \frac{\pi d^2}{4}\right)_{Fp} + \left(8\mu k\, D \cdot \frac{h_m + \frac{h}{2}}{D^2 - d^2} \cdot \frac{D^2}{d^2} \cdot \frac{\pi d^2}{4}\right)_{Fm} + \left[2k \cdot \frac{\pi d^2}{4} \cdot \left(1 + \frac{\mu d}{H}\right)\right]_{Fr} +$$

$$\left(2k \cdot \frac{D^2}{d^2} \cdot \frac{\pi d^2}{4} \ln \frac{D^2}{D^2 - d^2}\right)_{Fdef} \quad (3)$$

Where, $k$ is the maximum stress, $D$ is the diameter of container, $d$ is diameter of stamp head, $h_p$ is the height of the stamp, $h_m$ is length of extruded work piece behind the stamp, $H$ is the height of non-deformed work piece (Socaciu, 2014) and $h$ is defined:

$$h = \frac{D+d}{2} \frac{\sqrt{D^2 - d^2}}{d} \quad (4)$$

Using the indirect extrusion modelling methodology, the upper bound limits of the total HF2V device forces can be calculated from the sum of upper limits of friction forces from lead-bulge ($F_{f\_blg}$), lead-shaft ($F_{f\_sh}$) and lead-wall ($F_{f\_wall}$) interactions, compression forces ($F_{comp}$), deformation forces ($F_{def}$) and extrusion force ($F_{ext}$) from area reduction. Equation (3) is modified by matching the geometric parameters of the HF2V devices, shown in Figure 2, given as Equation (5):

$$F_{UB,indirect} = F_{comp} + F_{def} + F_{f\_blg} + F_{f\_wall} + F_{f\_sh} + F_{ext} \quad (5)$$

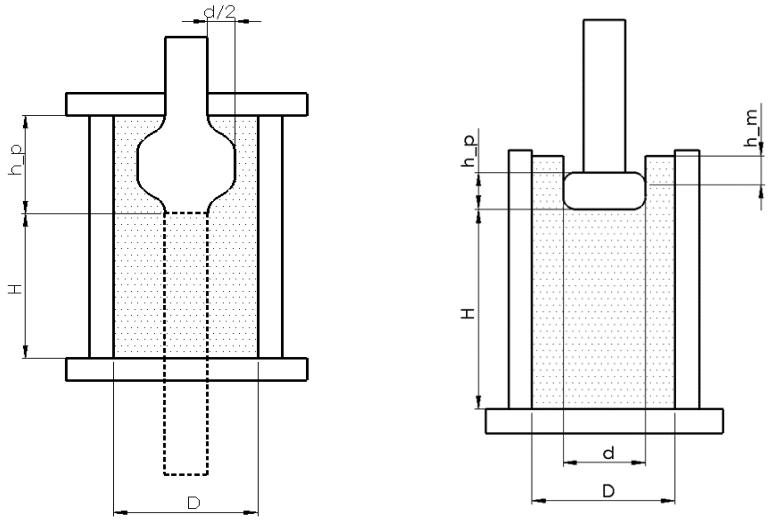


Figure 2: Geometric mapping of parts onto HF2V devices

The expression for compressive forces for HF2V devices is defined:

$$F_{comp} = 2Y_o\left(1+\mu\frac{D_{blg}-D_{sh}}{L_{cyl}-L_{blg}}\right)\frac{\pi\,(D_{blg}-D_{sh})^2}{4} \tag{6}$$

The deformation forces are defined:

$$F_{def} = 2Y_o\,\frac{{D_{cyl}}^2}{(d)^2}\,\frac{\pi\,d^2}{4}\,\ln\frac{{D_{cyl}}^2}{{D_{cyl}}^2-(D_{blg}-D_{sh})^2} \tag{7}$$

The force produced from the friction between the bulged shaft and the working material is calculated:

$$F_{f\_blg} = 8\mu Y_o\,\frac{(L_{blg})}{D_{blg}-D_{sh}}\,\frac{\pi\,(D_{blg}-D_{sh})^2}{4}\,\frac{{D_{cyl}}^2}{{D_{cyl}}^2-(D_{blg}-D_{sh})^2} \tag{8}$$

The working material flows against the wall creating friction forces between the wall and lead, defined:

$$F_{f\_wall} = 8\mu Y_o\,\frac{L_{blg}+{}^{h}/_{2}}{{D_{cyl}}^2-(D_{blg}-D_{sh})^2}\,\frac{\pi\,(D_{blg}-D_{sh})^2}{4}\,\frac{{D_{cyl}}^2}{{D_{cyl}}^2-(D_{blg}-D_{sh})^2} \tag{9}$$

Where, h is defined:

$$h = \frac{D_{cyl}+(D_{blg}-D_{sh})}{2}+\frac{\sqrt{{D_{cyl}}^2-{D_{sh}}^2}}{2} \tag{10}$$

Friction force produced by friction between the lead and no bulge shaft is determined by:

$$F_{f\_sh} = m\pi D_{sh}\frac{Y_o}{\sqrt{3}}(L_{cyl}-L_{blg}) \tag{11}$$

Pure extrusion forces ($F_{ext}$) is calculated by Equation (1).

## 4 ANALYSIS

The LB and UB models in are applied to 15 HF2V lead extrusion dampers whose experimental test data and geometric dimensions and yield stress ($Y_o$ ) are presented in Table 1. The yield stresses ($Y_o$) for pure lead at different reduction percentages in compression at 20 °C is considered for HF2V devices. $Y_o$ for pure lead in

compression for different reduction percentages of lead between the bulge and the cylinder walls (Loizou, 1953).

*Table 1:– HF2V parameters and yield stress ($Y_o$) values of pure lead used for LB and UB modelling.*

| Devices | Percentage Reduction (%) | $Y_o$ (N/mm$^2$) | $L_{cyl}$ (mm) | $L_{blg}$ (mm) | $D_{cyl}$ (mm) | $D_{blg}$ (mm) | $D_{shaft}$ (mm) |
|---|---|---|---|---|---|---|---|
| 1 | 17 | 23.17 | 110 | 30 | 89 | 40 | 30 |
| 2 | 34 | 29.30 | 110 | 30 | 89 | 50 | 30 |
| 3 | 47 | 32.43 | 110 | 30 | 89 | 58 | 30 |
| 4 | 28 | 27.80 | 130 | 30 | 66 | 40 | 30 |
| 5 | 56 | 33.91 | 130 | 30 | 66 | 50 | 30 |
| 6 | 40 | 32.43 | 50 | 23.3 | 50 | 32 | 20 |
| 7 | 40 | 32.43 | 70 | 20 | 50 | 32 | 20 |
| 8 | 42 | 32.43 | 100 | 30 | 50 | 35 | 24 |
| 9 | 33 | 30.89 | 160 | 20 | 60 | 42 | 33 |
| 10 | 42 | 32.43 | 100 | 23 | 50 | 35 | 24 |
| 11 | 45 | 32.43 | 75 | 30 | 70 | 48 | 30 |
| 12 | 21 | 26.26 | 160 | 20 | 54 | 35 | 30 |
| 13 | 25 | 27.03 | 160 | 20 | 54 | 36 | 30 |
| 14 | 33 | 30.89 | 160 | 20 | 54 | 38 | 30 |
| 15 | 35 | 31.00 | 100 | 17.2 | 40 | 27 | 20 |

The following assumptions are made for the UB analysis:

i. The friction coefficient ($\mu$) is $\mu = 0.25$, and assumed constant at all points of interaction between the lead and shaft surfaces.
ii. The forces of compression behind the bulge slope after extrusion are neglected.
iii. The velocity of the shaft relative to the outer casing is assumed to be 0.5mm /s for all the devices.
iv. The extrusion is assumed to occur at 20°C and the variation in temperature.

The yield strength is considered twice the average flow stress ($\bar{Y}$) (Groover, 2013), and defined:

$$Y_o = 2\bar{Y} \tag{13}$$

The flow stress is the value stress when the metal starts to flow plastically, defined:

$$\bar{Y} = \frac{K\varepsilon}{1+n} \tag{14}$$

Where, $K$ is the strength coefficient, and $n$ is the strain-hardening component. $K = 26.4$ and $n = 0.28$ for commercially pure lead (Wong et al., 1999). The corresponding $Y_o$ values calculated are given in Table 3. $\varepsilon$ is the strain during the deformation process defined:

$$\varepsilon = \frac{D_o - D_f}{D_o} \tag{15}$$

Where,

$$D_o = \frac{D_{cyl} - D_{sh}}{2} ; D_f = \frac{D_{cyl} - D_{blg}}{2} \quad (16)$$

The friction factor, m = 0.86 and is calculated using the following relationship (Bakhshi-Jooybari, 2002; Molaei et al., 2014):

$$m = 2\,\mu\sqrt{3} \quad (17)$$

A total of 15 HF2V experimental device forces ($F_{exp}$) are compared against the estimated upper bound and lower bound forces. The resulting LB and UB forces are compared to the peak forces from experimental tests. The experimental forces are expected to lie between the LB and UB forces.

LB and UB models provide a rough estimation of a broad range of maximum and minimum expected forces from HF2V devices. For practical applications, it will be helpful in determining device design forces. Mean UB and LB model forces are calculated based on the models presented and error based on experimental forces are calculated to determine the precise HF2V device forces.

*Table 2: The shear yield strength values of pure lead*

| Devices | $\varepsilon$ | $Y_o$ (N/mm$^2$) |
|---|---|---|
| 1 | 0.17 | 25.09 |
| 2 | 0.34 | 30.47 |
| 3 | 0.47 | 33.48 |
| 4 | 0.28 | 28.82 |
| 5 | 0.56 | 34.99 |
| 6 | 0.40 | 31.92 |
| 7 | 0.40 | 31.92 |
| 8 | 0.42 | 32.42 |
| 9 | 0.33 | 30.33 |
| 10 | 0.42 | 32.42 |
| 11 | 0.45 | 32.99 |
| 12 | 0.21 | 26.59 |
| 13 | 0.25 | 27.98 |
| 14 | 0.33 | 30.33 |
| 15 | 0.35 | 30.74 |

## 5 RESULTS AND DISCUSSION

Experimental HF2V device forces are compared to LB and UB estimates of HF2V devices using Equations (1) & (5) in Table 3. The lower bound model forces $F_{LB}$ are lower than all the experimental forces and the results from the indirect extrusion model shows the upper bound forces ($F_{UB,indirect}$) are greater than the experimental forces for all 15 devices, as expected.

The UB model over-estimates the device forces by 12-56% and the LB model under-estimates the HF2V forces by 28-57%. The $F_{UB,indirect}$ and $F_{LB}$ values provide limits of operational range of HF2V devices based on device design parameters and deformation of lead in the devices by creating a tight bound for all devices.

*Table 3: Comparison of HF2V LB and UB model forces to experimental forces.*

| Devices | $F_{LB}$ (kN) | $F_{exp}$ (kN) | $F_{UB,indirect}$ (kN) |
|---|---|---|---|
| 1 | 106.1 | 205 | 290.7 |
| 2 | 168.2 | 305 | 461.0 |
| 3 | 224.3 | 395 | 610.1 |
| 4 | 130.6 | 210 | 297.9 |
| 5 | 199.9 | 350 | 461.1 |
| 6 | 55.3 | 130 | 174.5 |
| 7 | 68.0 | 150 | 184.4 |
| 8 | 96.6 | 155 | 242.1 |
| 9 | 174.1 | 260 | 338.4 |
| 10 | 96.6 | 155 | 227.2 |
| 11 | 122.8 | 265 | 354.3 |
| 12 | 132.9 | 185 | 249.9 |
| 13 | 141.0 | 200 | 265.0 |
| 14 | 156.6 | 270 | 302.6 |
| 15 | 69.7 | 125 | 150.4 |

The precise device forces for the HF2V devices are estimated by calculating the mean between the UB and LB forces of the corresponding devices. The precise HF2V device forces are given in Table 4. The error is calculated for the average model forces and the experimental forces from the devices. The overall results from this calculation shows absolute errors ranging from ~1% to ~16% for all the model mean forces.

*Table 4: Mean UB/LB HF2V forces and corresponding errors with respect to experimental device forces.*

| Devices | $F_{exp}$ (kN) | $F_{mean-UB/LB}$ (kN) | Absolute Error |
|---|---|---|---|
| 1 | 205 | 198.4 | 3% |
| 2 | 305 | 314.6 | 3% |
| 3 | 395 | 417.2 | 6% |
| 4 | 210 | 214.25 | 2% |
| 5 | 350 | 330.5 | 6% |
| 6 | 130 | 114.9 | 12% |
| 7 | 150 | 126.2 | 16% |
| 8 | 155 | 169.3 | 9% |
| 9 | 260 | 256.2 | 1% |
| 10 | 155 | 161.9 | 4% |
| 11 | 265 | 238.5 | 10% |
| 12 | 185 | 191.4 | 3% |
| 13 | 200 | 203.0 | 2% |
| 14 | 270 | 229.6 | 15% |
| 15 | 125 | 110.0 | 12% |

Figure 3 shows the experimental device forces plotted along with UB and LB forces from Table 3 and precise device forces from Table 4. The experimental devices forces and the precise device forces lie

between the UB and LB force ranges. The mean LB/UB HF2V device forces estimated by taking the average of UB and LB model forces lies very close to the experimental forces in Figure 2.

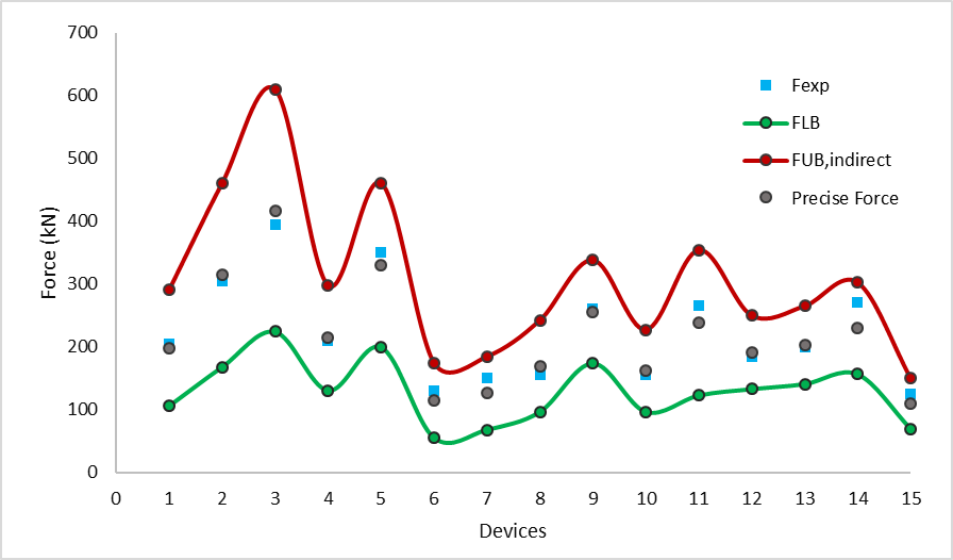


*Figure 3: $F_{exp}$ plotted along with UB and LB force ranges and precise forces for HF2V devices.*

## 6 CONCLUSION

This paper has presented a lower bound (LB) and an upper bound (UB) force modelling methods for HF2V devices by relating indirect extrusion parameters to HF2V lead extrusion devices. The UB models predict above the experimental force and the lower bound model predicts forces below the experimental device forces. The UB and LB model pair can be used to predict experimental device forces with absolute errors between 1-16%.

## 7 ACKNOWLEDGEMENTS

This project was supported by a Rutherford Discovery Fellowship, funded by the Ministry of Business, Innovation and Employment (MBIE) and administered by the Royal Society Te Apārangi, and by QuakeCoRE, a New Zealand Tertiary Education Commission-funded Centre. This is QuakeCoRE publication number 0655.

## 8 REFERENCES

Amini Hosseini, K., Hosseinioon, S., & Pooyan, Z. (2013). An investigation into the socioeconomic aspects of two major earthquakes in Iran. *Disasters, 37*(3), 516-535.

Bakhshi-Jooybari, M. (2002). A theoretical and experimental study of friction in metal forming by the use of the forward extrusion process. *Journal of materials processing technology, 125*, 369-374.

Dorahy, M. J., Renouf, C., Rowlands, A., Hanna, D., Britt, E., & Carter, J. D. (2016). Earthquake aftershock anxiety: An examination of psychosocial contributing factors and symptomatic outcomes. *Journal of loss and trauma, 21*(3), 246-258.

Drucker, D., Prager, W., & Greenberg, H. (1952). Extended limit design theorems for continuous media. *Quarterly of applied mathematics, 9*(4), 381-389.

Groover, M. P. (2013). *Principles of Modern Manufacturing: SI Version*. Wiley.

Horrobin, D., & Nedderman, R. (1998). Die entry pressure drops in paste extrusion. *Chemical Engineering Science, 53*(18), 3215-3225.

Hosford, W., & Caddell, R. (2007). *Mechanics and Metallurgy*. Cambridge University Press. https://doi.org/https://doi.org/10.1017/CBO9780511811111.009

King, S. A., Kiremidjian, A. S., Basöz, N., Law, K., Vucetic, M., Doroudian, M., Olson, R. A., Eidinger, J. M., Goettel, K. A., & Horner, G. (1997). Methodologies for evaluating the socio-economic consequences of large earthquakes. *Earthquake Spectra, 13*(4), 565-584.

Latham, D., Reay, A. M., & Pampanin, S. (2013, 21-22 February 2013). Kilmore street medical centre: Application of a post-tensioned steel rocking system. Steel Innovations Conference 2013, Christchurch, New Zealand.

Latham, D. A., Reay, A. M., & Pampanin, S. (2013). Kilmore Street Medical Centre: Application of an Advanced Flag-Shape Steel Rocking System. [ http://www.nzsee.org.nz/db/2013/Paper_3.pdf]. New Zealand Society for Earthquake Engineering–NZSEE–Conference, Wellington, New Zealand.

Loizou, N., Sims, R.B. (1953). The yield stress of pure lead in compression. *Journal of the Mechanics and Physics of Solids, 1*(4), 234-243.

Molaei, S., Shahbaz, M., & Ebrahimi, R. (2014). The relationship between constant friction factor and coefficient of friction in metal forming using finite element analysis. *Iranian Journal of Materials Forming, 1*(2), 14-22.

Rodgers, G. W. (2009). *Next Generation Structural Technologies: Implementing High Force-to-Volume Energy Absorbers* [Ph.D. thesis, University of Canterbury, Christchurch, New Zealand, Ph.D. thesis]. ⟨http://ir.canterbury.ac.nz/handle/10092/2906

Rodgers, G. W., Chase, J.G.,Mander, J.B. (2019, 2019). Repeatability and High-Speed Validation of Supplemental Lead-Extrusion Energy Dissipation Devices. *Advances in Civil Engineering, Vol 2019*, 13, Article 7935026. https://doi.org/http://dx.doi.org/10.1155/2019/7935026

Rowe, G. W. (1979). *Elements of metalworking theory*. Hodder Arnold.

Shannon, T. (2019, 10-12 October 2019). Turanga Library Christchurch - Hybrid Rocking Precast Concrete Wall Panels. Concrete New Zealand Conference, Dunedin.

Shinozuka, M., Rose, A., & Eguchi, R. (1998, 1998). *Engineering and socioeconomic impacts of earthquakes*. Multidisciplinary Center for Earthquake Engineering Research.

Socaciu, T. (2014). An analysis regarding the variation of necessary force by the indirect extrusion processes. *Procedia Technology, 12*, 433-438.

Symons, D. D., Chen, J., & Alton, P. (2014). Calculation of optimal jaw geometry for an electronic bond pull test. *Proceedings of the Institution of Mechanical Engineers, Part C: Journal of Mechanical Engineering Science, 228*(11), 1847-1858.

Vishnupriya, V., Rodgers, G. W., Mander, J. B., & Chase, J. G. (2018, Jun). Precision Design Modelling of HF2V Devices. *Structures, 14*, 243-250. https://doi.org/10.1016/j.istruc.2018.03.007

Wong, S., Hodgson, P. D., & Thomson, P. F. (1999). Room temperature deformation and recrystallisation behaviour of lead and lead–tin alloys in torsion and plane strain compression. *Materials science and technology, 15*(6), 689-696.

Xu, J., Xie, L., Li, B., Li, N., & Yang, Y. (2012). Anxiety symptoms among children after the Wenchuan earthquake in China. *Nordic journal of psychiatry, 66*(5), 349-354.